Energy-efficient communication in mobile aerial relay-assisted networks using predictive control ⋆

Omar J. Faqir * **Yuanbo Nie** ** **Eric C. Kerrigan** *,** **Deniz Gündüz** *

* *Department of Electrical & Electronic Engineering, Imperial College London, SW7 2AZ London, U.K. (e-mails: omar.faqir12@imperial.ac.uk;e.kerrigan@ic.ac.uk;d.gunduz@ic.ac.uk).*
** *Department of Aeronautics, Imperial College London, SW7 2AZ London, U.K. (e-mail: yuanbo.nie16@imperial.ac.uk)*

Abstract: Energy-efficient communication in wireless networks of mobile autonomous agents mandates joint optimization of both transmission and propulsion energy. In Faqir et al. (2017) we developed communication-theoretic data transmission and Newtonian flight mechanics models to formulate a nonlinear optimal control problem. Here we extend the previous work by generalizing the communication model to include UAV-appropriate slow fading channels and specifically investigate the potential from joint optimization of mobility and communication over a multiple access channel. Numerical results exemplify the potential energy savings available to all nodes through this joint optimization. Finally, using the slow fading channel problem formulation, we generate a chance-constrained nonlinear model predictive control scheme for control of a terrestrial network served by a single UAV relay. Closed-loop simulations are performed subject to uncertainties in both transmission and mobility models.

Keywords: Autonomous mobile robots, Communication networks, Information capacity, Model-based control, Nonlinear control, Optimal control

1. INTRODUCTION

Energy consumption remains a limiting factor for unmanned aerial vehicles (UAVs), where significant energy use comes from transmission and propulsion systems. In previous work (Faqir et al., 2017) we developed communication-theoretic and Newtonian dynamic models to represent the data transmission and locomotion efforts of agents. These models are used to formulate a nonlinear optimal control problem (OCP) with the objective of minimizing network energy expenditure. Here we generalize the communication model in the OCP to allow either additive white Gaussian noise (AWGN) or slow fading channels. For numerical simulations we consider the use of UAVs as enabling relays in disconnected terrestrial networks. In doing so, we provide validations and comparisons of our proposed solution against more naive communication policies. Unlike works that investigate the use of model predictive control (MPC) for control *over* mobile communication networks (e.g. networked control subject to communication constraints (Lavaei et al., 2008)), we consider the use of MPC for control *of* communication networks, or the control of data transfer throughout a mobile network.

To capture the cost of communication, it is important to define a node's communication energy as the sum of transmission energy and any propulsion energy used for facilitating transmission, e.g. when a UAV speeds up or slows down to maintain better channel access. The network's energy expenditure is the sum of each node's communication energy. We consider a network consisting of a set of data-generating source nodes (such as a remote sensor network), which are geographically separated from an infrastructure-connected access point (AP). A mobile UAV relays data between the source network and the AP, as shown in Figure 1. Since both the source network and UAV operate on local energy reserves, energy-efficient relaying operation requires joint optimization of the source's transmission energy and the relay's propulsion energy. This is pertinent for

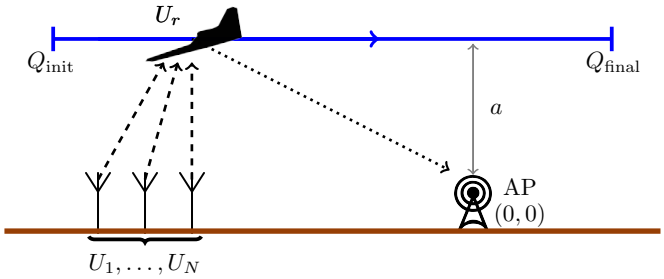

Fig. 1. Simulation geometry consisting of UAV relay U_r, access point U_0 and N source nodes. U_r flies at an altitude $a = 1000\,\text{m}$ with no lateral displacement. Dashed lines show multiple access uplinks from sources to U_r. The single access download from U_r to the AP is shown by a dotted line.

⋆ The support of the EPSRC Centre for Doctoral Training in High Performance Embedded and Distributed Systems (HiPEDS, Grant Reference EP/L016796/1) is gratefully acknowledged.

the source network that — as in the case of a remote sensor network — may have long lifetime requirements. Trajectories generated by the proposed OCP exhibit potential network level energy savings upwards of 30%. Closed-loop simulations motivate including robust channel models into the OCP formulation.

Communication-theoretic bounds, similar to those employed by us in Faqir et al. (2017) and in this paper, are used by Zeng et al. (2016); Lyu et al. (2016); Zeng and Zhang (2016). Zeng et al. (2016) consider using a single UAV relay to maximize data throughput between a stationary source-sink pair. For a fixed trajectory, the optimal transmission scheme is a directional water filling from source to sink. A cyclical multiple access scheme is used by Lyu et al. (2016) to maximize the throughput of a set of ground terminals served by a UAV relay.

For communication in networks of rolling robots, Yan and Mostofi (2012) develop a model for channel fading dynamics in indoor environments. Ali et al. (2015, 2016) use this model, with a realizable propulsion model for rolling-robots, in order to minimize communication energy.

2. PROBLEM FORMULATION

As may be seen in Figure 1, there exists N stationary data-generating sources $U_n, n \in \mathcal{N} \triangleq \{1, \ldots, N\}$, which are geographically separated from a stationary access point (AP) U_0 located at the position $(0, 0, 0)$ in Cartesian space. Consider a single UAV relay U_r, $r = N + 1$, traveling over a time period $\mathcal{T} \triangleq [0, T]$ in a linear trajectory, denoted $X_r : t \mapsto (q(t), 0, a)$. Assumption on linear trajectories confines the motion of U_r to a single dimension, with constant altitude a and no lateral displacement. The use of fixed linear paths does not detract form our results, since most path planning algorithms operate over a sufficiently long time horizon and are generally restricted to be either linear or circular (Sujit et al., 2014). For example, Kang and Hedrick (2009) use nonlinear model predictive control (NMPC) for robust tracking of linear trajectories by fixed wing UAVs.

U_r receives data from $U_n, n \in \mathcal{N}$, to be forwarded to the AP by time T. For notational simplicity, but also motivated by the optimal UAV path described in Zeng et al. (2016), we restrict sources to be located on ground at positions $X_n \triangleq (q_n, 0, 0)$, such that the relay travels directly over all source nodes. Over the interval $\mathcal{T}$, U_r must travel from position $q(0) = Q_{\text{init}}$ to $q(T) = Q_{\text{final}}$.

Denote the set of transmitting nodes (both source and relay) as $\mathcal{M} \triangleq \mathcal{N} \cup \{r\}$. The data received by the relay is stored in an on-board memory before being forwarded to the AP. Let $s_r(t)$ denote the amount of data stored in the relay's data buffer at time t. We require $s_r(t) \leq M, \forall t \in \mathcal{T}$, where M is the size of the relay's on-board memory in bits. The buffers of all transmitting nodes are subject to the following initial and final conditions:

$$s_n(0) = D_n, \qquad s_n(T) = 0, \forall n \in \mathcal{N} \tag{1}$$

$$s_r(0) = 0, \qquad s_r(T) \leq D_r, \tag{2}$$

while the AP U_0 is modeled as an ideal (infinite) sink, and is not subject to capacity constraints. We allow for $D_r \neq 0$ to simulate U_r as a mobile sink ($D_r = M = \infty$).

2.1 Communication Model

Nodes $U_m, m \in \mathcal{M}$, are assumed to have a single omnidirectional antenna capable of transmitting at a maximum power $P_{\max}$. Wireless communication links exist between nodes $U_m, U_n, \forall m \in \mathcal{M}, n \in \{0, r\}$ over channels with corresponding gain $h_m \triangleq \nu_m^2$, where ν_m is a realization of a random variable corresponding to the channel distribution. The signal gain across a link is defined as

$$\eta(\chi_{nm}(t), h_m) \triangleq \frac{h_m G}{\chi_{nm}(t)^\alpha}, \tag{3}$$

where $G = \tilde{G} d_0^\alpha$ is a unitless constant representing transmit and receive antenna gains and path loss $\tilde{G}$ at the reference distance d_0. $\alpha > 1$ is the path loss exponent, and

$$\chi_{nm}(t) \triangleq \|X_{nm}(t)\|^2 = \|(q_{nm}(t), 0, a)\|^2, \tag{4}$$

where $q_{nm}(t) \triangleq q_n(t) - q_m(t)$. The modeled network consists of two orthogonal frequency bands B_r and B_A, respectively dedicated for source-to-relay and relay-to-AP transmissions. In doing so, we assume that no direct link exists from the sources to the AP — e.g., due to physical barriers on the ground — thereby rendering the mobile terminal essential for relaying data through two-hop communication. Due to the lack of direct links, it is optimal for the relay to first decode the data transmitted by the source nodes, and then re-encode and forward them to the destination; that is, the relay adopts the so-called decode-and-forward protocol (Gündüz et al., 2010). We now consider two different channel modeling regimes.

Additive white Gaussian noise (AWGN): All links are modeled as AWGN channels with zero-mean unit-variance independent noise components. We evaluate the achievable data rates using Shannon capacity, which serves as an upper bound on the achievable rates subject to average power constraints.

The uplink from the sources to the relay forms a Gaussian multiple access channel (MAC), for which the set of achievable rate tuples is defined by a polymatroid capacity region (Tse and Viswanath, 2005). At any instance, $U_n, n \in \mathcal{N}$, can transmit to relay node U_r at a non-negative data rate ϱ_n using an associated transmission power p_n. The capacity region $\mathcal{C}_N(\cdot)$ of the MAC formed by the source nodes transmitting to the relay node denotes the set of all achievable rate tuples ϱ, and is bounded by $2^N - 1$ nonlinear constraints. We define this as

$$\mathcal{C}_N(\chi, p, h) \triangleq \{\varrho \geq 0 \mid f(\chi, p, \varrho, h, \mathcal{S}) \leq 0, \forall \mathcal{S} \subseteq \mathcal{N}\}, \tag{5}$$

where χ is the tuple of χ_{rn}, defined in (4), $p \in \mathcal{P}^N$ is the tuple of transmission powers allocated by the N users on this channel, $\mathcal{P} \triangleq [0, P_{\max}]$ is the range of possible transmission powers for each user, and $f(\cdot)$ is a nonlinear function defined as:

$$f(\chi, p, \varrho, h, \mathcal{S}) \triangleq \sum_{n \in \mathcal{S}} \left(\varrho_n - B_r \log_2 \left(1 + \sum_{n \in \mathcal{S}} \eta_{rn}(\chi_{rn}, h_n) p_n \right) \right), \tag{6}$$

where B_r is the channel bandwidth allocated to the relay, ϱ_n is the n^{th} component of ϱ, and channel gain $h_n = 1, \forall n \in \mathcal{N}$ for AWGN channels.

$\mathcal{C}_N$ is bounded from above by $2^{\text{card}(\mathcal{N})}-1$ nonlinear functions. The exponential growth in the number of constraints upper bounding $\mathcal{C}_N$ is computationally intractable, limiting the number of nodes using each MAC. This is often the case in small, or highly structured networks where only small subsets of nodes access each MAC. In practice, transmitting at arbitrary rate tuples in the capacity region can be achieved through successive interference cancellation (SIC) and time-sharing or message splitting (Tse and Hanly, 1998).

The rate from the relay to the AP is bounded using a similar function:

$$g(\chi_r, p_r, \varrho_r, h_r) \triangleq \varrho_r - B_A \log_2\left(1+\eta(\chi_r, h_r)p_r\right). \quad (7)$$

Importantly, for an AWGN channel, all rates determined by (6) and (7) may be achieved with arbitrarily small probability of error.

Slow Fading Channel: In a slow fading channel, the actual channel gains are constant but random over a single transmission interval, and as such are no longer modeled by $h_n = 1$. Considering (6) with random vector h, it is now possible that $\mathcal{C}_{\mathcal{N}} = \emptyset$ with nonzero probability regardless of the transmission power and distance (assuming channel state is unknown at the transmitter, hence power allocation is not possible). Therefore, it is impossible to guarantee successful transmission at any strictly positive rate with zero probability of error (Tse and Viswanath, 2005), and it is no longer beneficial to model the relation between rates, power and distance through ergodic capacity.

Often the channel distribution is known, even if the actual realization h is unknown. In this case, we may define a more useful performance measure, the $\epsilon-$*outage capacity* $\mathcal{C}_N^\epsilon$, which is the set of achievable rates that can guarantee a maximum outage probability of ϵ, defined as

$$\mathcal{C}_N^\epsilon \triangleq \mathcal{C}\left(\chi, p, \Gamma^{-1}(1-\epsilon)\right), \quad (8)$$

where Γ is the complementary cumulative distribution of h, $\Gamma(x) \triangleq \Pr\{h \geq x\}$ (Tse and Viswanath, 2005). Rates are now determined such that $(\varrho_1, \ldots, \varrho_N) \in \mathcal{C}_N^\epsilon$, and

$$\mathcal{C}_N^\epsilon \subset \mathcal{C}_N \quad (9)$$

with high probability. In doing so, we are performing chance-constrained optimization. However, because the probability density of the stochastic variable h is known, the problem may be written in a deterministic form, with no additional complexity (Schwarm and Nikolaou, 1999). The slow fading channel model naturally allows for a chance constrained OCP. Future work may instead consider achieving robust control through optimization over feedback policies.

2.2 Propulsion Energy Model

Mozaffari et al. (2017) determine the energy required for a rotary craft to move between locations at a fixed speed as a linear combination of the decoupled vertical and horizontal powers. This is not necessarily the case for a fixed-wing craft. Zeng and Zhang (2016) also use a Newtonian basis, modeling drag forces as consisting of parasitic drag (proportional to the square of the speed) and lift-induced drag (inversely proportional to the square of the speed).

The fixed-wing UAV U_r is restricted to moving at positive speeds $v \in \mathcal{V} \triangleq [V_{\min}, V_{\max}]$, where $0 < V_{\min} \leq V_{\max}$. We take a general approach, using Newtonian laws as a basis. In what follows next, $D(\cdot)$ models the resistive forces acting on U_r in accordance with the following assumption

Assumption 1. The resistive forces acting on U_r may be modeled by the function $v \mapsto D(v)$ such that $v \mapsto vD(v)$ is convex on the domain of admissible speeds $v \in \mathcal{V}$ and ∞ on $v \notin \mathcal{V}$.

The propulsion force $F(\cdot)$ generated by the UAV must satisfy the force balance equation

$$F(t) - D(v(t)) = ma(t), \quad (10)$$

where m is the mass of U_r, $v(t)$ is the speed and $a(t) = \dot{v}(t)$ is the acceleration along the direction of motion at time t. The instantaneous power used for propulsion is the product $v(t)F(t)$, with the total propulsion energy taken as the integral of power over time (Zeng and Zhang, 2016). We assume $v(t) > 0$, $\forall t \in \mathcal{T}$, valid for fixed-wing aircrafts.

Similar to Zeng and Zhang (2016) we use $D(\cdot)$ of the form

$$D(v) \triangleq \begin{cases} C_{D1}v^2 + C_{D2}v^{-2}, & \forall v \in \mathcal{V} \\ \infty, & \text{otherwise} \end{cases} \quad (11)$$

where the parasitic drag coefficient C_{D1} and lift induced drag coefficient C_{D2} follow from

$$C_{D1} \triangleq \frac{\psi C_{D0} S}{2}, \quad C_{D2} = \frac{2L^2}{(\pi e_0 A_R)\psi S}, \quad (12)$$

where ψ is the air density, C_{D0} is the base drag coefficient, S is the wing area, e_0 is the Oswald efficiency, and A_R is the wing aspect ratio. L is the induced lift, which for fixed-altitude flight must be equal to the craft weight $W = mg$. We use $C_{D1} = 9.26 \times 10^{-4}$ and $C_{D2} = 2250$, similar to Zeng and Zhang (2016).

The Newtonian constraint (10), being a nonlinear equality, and the propulsion power cost, being the product $F(t)v(t)$, are both non-convex. We substitute $F(t)$ from (10) into the energy integral, evaluating propulsion energy as

$$\int_0^T v(t)F(t)\mathrm{d}t = \underbrace{\int_0^T v(t)D(v(t))\mathrm{d}t}_{f_1(v)} + \underbrace{\frac{m}{2}\left(v^2(T) - v^2(0)\right)}_{f_2(v)}, \quad (13)$$

where $f_1(v)$ is convex by Assumption 1. $f_2(v)$ is the analytic evaluation of the change in kinetic energy, which is convex assuming fixed initial conditions $v(0)$. The proof may be found in Faqir et al. (2017).

2.3 Continuous-Time Optimal Control Problem

The tuple of describing variables (state and control variables) for sources $U_n, n \in \mathcal{N}$, is$Y_n \triangleq (p_n, \varrho_n, s_n)$ and relay is $Y_r \triangleq (p_r, \varrho_r, s_r, q_r, v, a)$. The continuous-time OCP is

$$\min_{Y_n, Y_r} \int_0^T \left(\sum_{n=1}^N \{p_n(t)\} + p_r(t) + v(t)D(v(t))\right)\mathrm{d}t + \frac{m}{2}\left(v^2(T) - v^2(0)\right) \quad (14a)$$

$$\text{s.t. } \forall n \in \mathcal{N}, m \in \mathcal{M}, t \in \mathcal{T}, \mathcal{S} \subseteq \mathcal{N}$$

$$f(q(t), p(t), \varrho(t), \tilde{h}, \mathcal{S}) \leq 0 \tag{14b}$$
$$g(q_{r0}(t), p_r(t), \varrho_r(t), \tilde{h}_r) \leq 0 \tag{14c}$$
$$ma(t) + D(v(t)) \leq F_{\max} \tag{14d}$$
$$\dot{s}_n(t) = -\varrho_n(t) \tag{14e}$$
$$\dot{s}_r(t) = -\varrho_r(t) + \textstyle\sum_{n=0}^{N} \varrho_n(t) \tag{14f}$$
$$\dot{q}(t) = \zeta v(t) \tag{14g}$$
$$\dot{v}(t) = a(t) \tag{14h}$$
$$s_n(0) = D_n, \quad s_n(T) = 0 \tag{14i}$$
$$s_r(0) = 0, \quad s_r(T) \leq D_r \tag{14j}$$
$$q(0) = Q_{\text{init}}, \quad q(T) = Q_{\text{final}} \tag{14k}$$
$$v(0) = v_{\text{init}}, \quad v(T) = v_{\text{final}} \tag{14l}$$
$$\underline{Y}_m \leq Y_m(t) \leq \bar{Y}_m. \tag{14m}$$

The cost function (14a) sums all transmission energies and the propulsion energy of the relay. Constraints (14b), (14c) respectively bound the achievable data rate of the MAC source-to-relay uplink, and the single access relay-to-AP downlink. $\tilde{h} = 1$ for AWGN channels and $\tilde{h} = \Gamma^{-1}(1 - \epsilon)$ for slow fading channels. (14d) upper bounds thrust with $F_{\max}$. The, now linear, system dynamics are included by (14e)–(14h). Constraints (14i)–(14l) provide boundary conditions for buffers, position and speed. The relay must reach its final destination by time $t = T$ without violating the force-acceleration constraint, which is implicit in the objective. Note that $\zeta \in \{-1, 1\}$, depending on whether the relay position $q(t)$ is decreasing or increasing, respectively, with speed $v(t) \geq 0$. (14m) includes simple bounds

$$\begin{aligned} \underline{Y}_n &= (0, 0, 0), & \underline{Y}_r &= (0, 0, 0, -\infty, V_{\min}, -\infty), \\ \bar{Y}_n &= (P_{\max}, \infty, \infty), & \bar{Y}_r &= (P_{\max}, \infty, M, \infty, V_{\max}, \infty), \end{aligned} \tag{15}$$

on decision variables, where $0 < V_{\min} \leq V_{\max}$. This problem is only feasible if there exists a trajectory admissible with respect to the aforementioned models and bounds. Consider the simple case of a mobile transmitter following an arbitrary linear path with reference to a stationary receiver. Even in the limit of $T \to \infty$, the maximum data transfer subject to transmission power constraints is finite. Therefore, in general we cannot guarantee existence of a feasible profile. Feasibility is assumed for simulations.

3. SIMULATION RESULTS

The continuous-time problem is formulated and solved using `ICLOCS2` (Nie et al., 2018b), through a `MATLAB` interface. `ICLOCS2` performs transcription to generate a discretized OCP, which is solved with the open source primal dual Interior Point solver `Ipopt v.3.12.4`. `ICLOCS2` allows for rate constraints to be directly implemented on the discretized mesh, to prevent singular arcs in solution trajectories as well as improving the computational efficiency (Nie et al., 2018a). We use this feature to place rate constraints on the acceleration. Constant parameters across all simulations are shown in Table 1.

Table 1. Model and simulation parameters.

σ^2 [W]	B [Hz]	M [GB]	$P_{\max}$ [W]	α [–]	T [min]
10^{-10}	10^5	1	100	1.5	20

(q_1, q_2) [km]	Q_{init} [km]	Q_{final} [km]	$(V_{\min}, V_{\max})$ [m/s]
$(-19.1, -14.3)$	-23.8	0	$(12, 28)$

Table 2. Transmission energy of source i (ϵ_i) and total network communication energy (ϵ_C) for UAV uplink under different schemes.

	Separate BW		Shared BW (MAC)	
	$v = v_{\text{avg}}$	$v = v^*$	$v = v_{\text{avg}}$	$v = v^*$
ϵ_C	NA	1	0.690	0.678
ϵ_1	NA	1	0.283	0.224
ϵ_2	NA	1	0.302	0.231

3.1 Open-loop Energy Savings

We perform open-loop simulations assuming ideal AWGN channels to compare the potential energy savings. There exist source nodes $U_{1,2}$, which must offload all data to a receiving UAV U_r. The UAV operates as an ideal sink with no memory constraints, $M = D_r = \infty$. Sources are initialized with a starting data load $D_1 = D_2 = 25\,\text{MB}$. Communication occurs over a two-user MAC, where the set of achievable rate tuples is upper bounded by three functions of the form (6). This is the first result to combine mobility with transmission over a MAC.

We construct comparative schemes using the following physical network constraints. Firstly, resources may be partitioned such that there is no inter-user interference. Therefore U_1, U_2 transmit on single access channels (SAC) of designated bandwidth $B_1 = B_2 = B_r/2$. Partitioning B is computationally simpler, since the number of constraints scale linearly, rather than exponentially with the number of source nodes. Secondly, optimization of transmission policy may be performed subject to fixed UAV trajectory. In this case we assume that U_r moves at constant speed $v_{\text{avg}} = (Q_{\text{final}} - Q_{\text{init}})/T$, using minimal propulsion energy. Combining these constraints gives four possible protocols.

Table 2 shows a comparison of the total energy usage ϵ_C, equivalent to the cost function (14a), and the transmission energy ϵ_1, ϵ_2 used by source nodes in each scheme. All energies are given as a percentage of the worst case feasible scenario. In the simplest case, where U_1, U_2 operate on an SAC and U_r moves at a fixed speed, the optimal transmission policy of each node is a water-filling solution, determined by a single water-filling parameter (Tse and Viswanath, 2005). This reduces the infinite dimensional search space of the original OCP to a single dimension. However, for the given starting data load, the problem is infeasible under these conditions. Generating a solution by solving (14) results in a 32% total energy savings when compared with joint optimization over single access channels, while sources U_1, U_2 each use approximately 76% less transmission energy. Although there is not significant total network energy savings for the MAC uplink under different speed regimes, both U_1, U_2 respectively save 20.8% and 23.51% transmission energy by allowing the relay to vary speed. This may be of particular importance in remote sensing applications, where source nodes may have stringent energy requirements or perform energy harvesting.

3.2 Closed-loop Simulation

For closed-loop simulation, an NMPC control policy is generated by resolving (14) at each computation interval $t_c = 10\,\text{s}$, subject to initial conditions set by measured

data. We consider the geometry seen in Figure 1, where sources U_1, U_2 are initialised with $D_1 = D_2 = 11\,\text{MB}$ and U_r has a finite memory constraint of $M = 1.5D_1$. All data must be relayed to the AP by time T. The finite-time nature of the experiment motivates the use of decreasing horizon control, where the final time is constant and the horizon length is reduced at each t_c. The NMPC problem is solved centrally, with full state information. In practice, position and velocity information is found as a combination of GPS and IMU data.

Typically data is encoded and transmitted in discrete codewords over packet intervals $t_p \ll t_c$. At each computation interval the complete information at each node is encoded at a rate determined by (14). We assume a simple repeat request (ARQ) protocol, where transmitters get feedback through 1 bit acknowledgement (ACK/NAK) signals. Storage buffers are only updated with successfully decoded information. Information in an unsuccessfully decoded codeword is entirely retransmitted at a later time.

The network operates over slow fading channels, where channel realizations are random but constant over t_p. We therefore formulate (14) with ϵ-outage capacity constraints, ensuring the control policy is robust to channel realizations. In the following we consider the MAC channel over a single codeword interval, dropping time dependency in notation. For actual realization $\tilde{h}_n$, channel outage — where the codeword is not successfully decoded — occurs because one or more of the received powers $\tilde{\beta}_n \triangleq \eta(\chi_{rn}, \tilde{h}_n)p_n$ was smaller than predicted and cannot support rate ϱ_n. The decoder may perform joint decoding of received signals, or decode a subset of received signals, treating others as interference. Precisely, for an N-user MAC, information transmitted from users in $\mathcal{S} \subseteq \mathcal{N}$ is successfully decoded if

$$\frac{\sum_{m\in\mathcal{M}} \beta_m}{1+\sum_{j\in\mathcal{S}'} \beta_j} \geq \frac{\sum_{m\in\mathcal{M}} \tilde{\beta}_m}{1+\sum_{j\in\mathcal{S}'} \tilde{\beta}_j}, \forall \mathcal{M} \subseteq \mathcal{S}, \qquad (16)$$

where $\mathcal{S}' \triangleq \mathcal{N} \setminus \mathcal{S}$ and $\beta_i \triangleq \eta(\chi_{rm}, \Gamma^{-1}(1-\epsilon))p_m$. For a single user channel, this simplifies to $\varrho_r \geq \tilde{\varrho}_r$. Since the rate tuple generated by problem (14) is always on the boundary of the capacity region (Faqir et al., 2017), (16) is only a function of transmission powers and not rates.

UAVs are advantageous in communication networks due to line of sight (LoS) links. Multipath scattering may still occur, such as off objects near ground nodes or flight surfaces of the UAV. Rician fading is suitable for modelling received signal strength in channels with strong LoS components (Zhou et al., 2012). For each channel used, ν is a vector of random variables drawn from a Rice distribution characterized by K-factor κ, defined as the ratio of received signal power in the LoS path to the power received from scattered paths. For $\kappa = \infty$ there is no fading and the model reduces to AWGN (Zhou et al., 2012). The cumulative distribution $\Gamma(\cdot)$ of a Rician channel is a Marcum Q-function of order 1. In our simulations $\kappa = 10$.

The UAV may also be disturbed by wind during flight. We model the disturbance entering the first derivative (Kang and Hedrick, 2009) such that ground speed $\dot{q}$ is the sum of air speed $\dot{v}$ and wind speed $\dot{w}$. To account for this, the system state is augmented with disturbance variable $\delta(t)$,

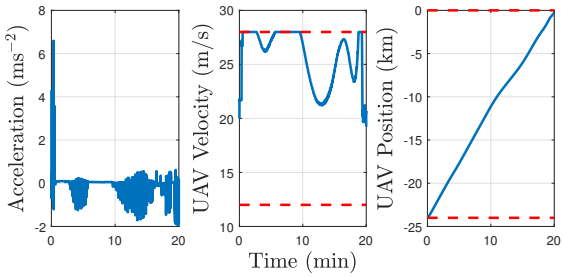

(a) U_r acceleration, velocity and displacement profiles.

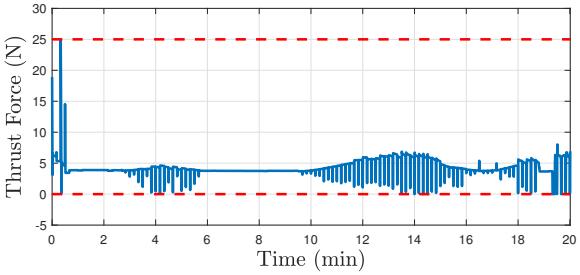

(b) U_r thrust profile.

Fig. 2. Mobility related state and input trajectories (solid lines) for U_r during UAV relay simulation. Dashed lines show constraints.

$$\dot{\delta}(t) = 0, \forall t \in \mathcal{T}, \delta(0) = w_{\text{meas}} \qquad (17)$$

and redefined position dynamics

$$\dot{q}(t) \triangleq \zeta v(t) - \delta(t). \qquad (18)$$

With full state information, the estimate $\dot{w}_{\text{meas}}$ is calculated with a moving average filter. In the following simulation $\dot{w} = -6\,\text{m/s}$.

Channel outages and wind disturbances means the finite time problem may be infeasible. In this case we switch to a variable horizon for the last few iterations (the convergence analysis of the variable time horizon OCP could be a topic of future work). Simulations are performed for $\Gamma^{-1}(1-\epsilon) \approx 0.2$, with results shown in Figures 2–3. Figure 2a shows the mobility dynamics of the UAV, where a velocity constraint becomes active as the UAV slows down to offload collected data to the AP. The extreme change in velocity results from the UAV memory s_r approaching capacity. Figure 2b shows the thrust required to maintain altitude during this maneuver. Since $C_{D2} \gg C_{D1}$ in (11), a wind speed of $\dot{w} = -6$ beneficially slows down the UAV, reducing the minimum energy by $\approx 31\%$ compared to a wind speed of $\dot{w} = 6$.

Commanded rates over t_c are strict upper bounds on achievable information transfer because, even for favorable channel realizations, data will not be transfered faster than predicted. Figures 3a–3b show data interchange between $U_i, i \in \{0, 1, 2, r\}$ in terms of the storage memory and achieved rates. Figure 3c shows the associated transmission power profile. Maximum power constraints are active while the UAV's buffer is close to capacity, during which the incoming and outgoing data from U_r are similar.

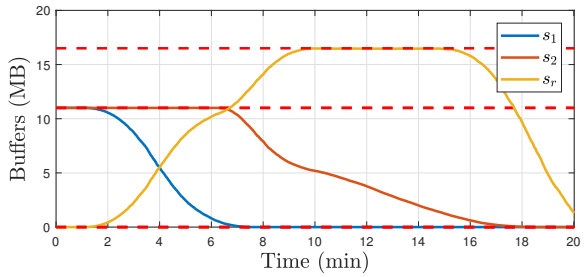

(a) Data storage buffers of U_1, U_2, U_r.

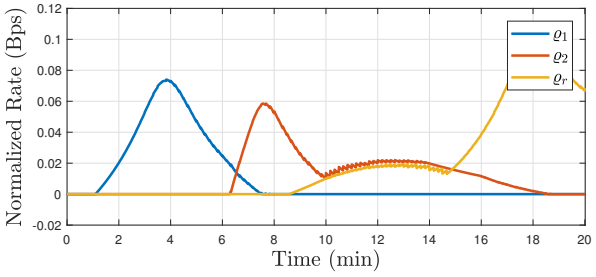

(b) Transmission data rates of $U_1, U_2.U_r$.

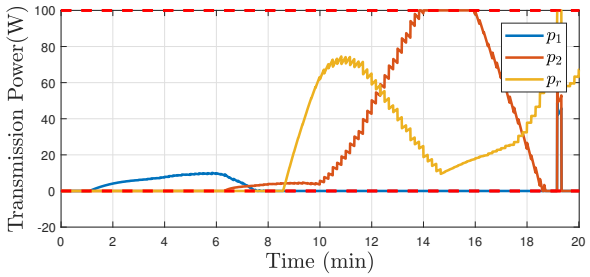

(c) Allocated transmission powers of U_1, U_2, U_r.

Fig. 3. Transmission related state/input trajectories (solid lines) for nodes U_1, U_2, U_r during UAV relay simulation. Dashed lines show hard constraints.

4. CONCLUSIONS

We have considered simultaneous optimization of propulsion and transmission energies for the particular geometry of a UAV relay-assisted communication network. A general optimal control problem for energy minimization was formulated based on dynamic models for both transmission and mobility. The chosen geometry exhibited the possibility of jointly optimizing node mobility along with transmission across a MAC. Open-loop simulations showed significant potential energy savings available with this method, with source nodes in particular saving upwards of 75% energy. Closed-loop simulations were performed, subject to significant communication channel uncertainty, motivating investigation into more realistic, potentially stochastic channel models and control laws.

REFERENCES

Ali, U., Cai, H., Mostofi, Y., and Wardi, Y. (2016). Motion and communication co-optimization with path planning and online channel estimation. *arXiv preprint arXiv:1603.01672*.

Ali, U., Yan, Y., Mostofi, Y., and Wardi, Y. (2015). An optimal control approach for communication and motion co-optimization in realistic fading environments. In *American Control Conference (ACC), 2015*, 2930–2935. IEEE.

Faqir, O.J., Kerrigan, E.C., and Gündüz, D. (2017). Joint optimization of transmission and propulsion in aerial communication networks. *arXiv preprint arXiv:1710.01529*.

Gündüz, D., Khojastepour, M.A., Goldsmith, A., and Poor, H.V. (2010). Multi-hop mimo relay networks: Diversity-multiplexing tradeoff analysis. *IEEE Trans. Wireless Comm.*, 9(5), 1738–1747.

Kang, Y. and Hedrick, J.K. (2009). Linear tracking for a fixed-wing UAV using nonlinear model predictive control. *IEEE Transactions on Control Systems Technology*, 17(5), 1202–1210.

Lavaei, J., Momeni, A., and Aghdam, A.G. (2008). A model predictive decentralized control scheme with reduced communication requirement for spacecraft formation. *IEEE Transactions on Control Systems Technology*, 16(2), 268–278.

Lyu, J., Zeng, Y., and Zhang, R. (2016). Cyclical multiple access in UAV-aided communications: A throughput-delay tradeoff. *IEEE Wireless Communications Letters*, 5(6), 600–603.

Mozaffari, M., Saad, W., Bennis, M., and Debbah, M. (2017). Mobile unmanned aerial vehicles (UAVs) for energy-efficient internet of things communications. *arXiv preprint arXiv:1703.05401*.

Nie, Y., , and Kerrigan, E.C. (2018a). How should rate constraints be implemented in nonlinear optimal control solvers? In *Proc. 6th IFAC Conference on Nonlinear Model Predictive Control*.

Nie, Y., Faqir, O.J., and Kerrigan, E.C. (2018b). ICLOCS2: Solve your optimal control problems with less pain. In *Proc. 6th IFAC Conference on Nonlinear Model Predictive Control*.

Schwarm, A.T. and Nikolaou, M. (1999). Chance-constrained model predictive control. *AIChE Journal*, 45(8), 1743–1752.

Sujit, P., Saripalli, S., and Sousa, J.B. (2014). Unmanned aerial vehicle path following: A survey and analysis of algorithms for fixed-wing unmanned aerial vehicles. *IEEE Control Systems*, 34(1), 42–59.

Tse, D. and Viswanath, P. (2005). *Fundamentals of wireless communication*. Cambridge university press.

Tse, D.N.C. and Hanly, S.V. (1998). Multiaccess fading channels. I. polymatroid structure, optimal resource allocation and throughput capacities. *IEEE Transactions on Information Theory*, 44(7), 2796–2815.

Yan, Y. and Mostofi, Y. (2012). Robotic router formation in realistic communication environments. *IEEE Transactions on Robotics*, 28(4), 810–827.

Zeng, Y. and Zhang, R. (2016). Energy-efficient uav communication with trajectory optimization. *arXiv preprint arXiv:1608.01828*.

Zeng, Y., Zhang, R., and Lim, T.J. (2016). Throughput maximization for mobile relaying systems. *IEEE Trans. Communications*, 64(12), 4983–4996.

Zhou, Y., Li, J., Lamont, L., and Rabbath, C.A. (2012). Modeling of packet dropout for UAV wireless communications. In *Computing, Networking and Communications (ICNC), 2012 International Conference on*, 677–682. IEEE.